이학석사 학위논문

머리 탑재형 초소형형광현미경을 이용한 전두대상피질에서의 통증과 가려움 처리에 관한 연구

Studies on pain and itch signal processing
in the anterior cingulate cortex
with head-mounted fluorescent microscope

2020년 8월

서울대학교 대학원
자연과학대학 생명과학부
오 지 혜

머리 탑재형 초소형형광현미경을 이용한 전두대상피질에서의 통증과 가려움 처리에 관한 연구

Studies on pain and itch signal processing in the anterior cingulate cortex with head-mounted fluorescent microscope

지도교수 강 봉 균

이 논문을 이학석사 학위논문으로 제출함

2020년 7월

서울대학교 대학원

자연과학대학 생명과학부

오 지 혜

오 지 혜의 이학석사 학위논문을 인준함

2020년 7월

위 원 장 김 형 (인)

부위원장 강 봉 균 (인)

위 원 이 용 석 (인)

Studies on pain and itch signal processing in the anterior cingulate cortex with head-mounted fluorescent microscope

Advisor. Professor Bong-Kiun Kaang

A dissertation submitted to the
Graduate Faculty of Seoul National University in
Partial fulfillment of the requirement for the
Degree of Master of Science

August 2020

Jihae Oh

Department of Biological Science
Graduate School of Natural Sciences
Seoul National University

CONTENTS

List of Figures

Abstract

Studies on pain and itch signal processing in the anterior cingulate cortex with head-mounted fluorescent microscope

Jihae Oh

Department of Biological Science

Graduate School of Natural Sciences

Seoul National University

Pain and itch sensations are different affective modes, and their transmission pathways and the brain areas processing them are intimately related to each other. Anterior cingulate cortex (ACC) has been known for its role in processing both pain and itch sensation. There are hypotheses explaining how the somatosensory modalities can be perceived as different ones in brain. However, it was barely studied how these two somatosensory stimuli would be processed in the same brain area. In this study, I figured out the ACC neurons were highly co-activated when received the itch and pain stimuli with 6h interval than 72h interval. Additionally, when inhibiting the pain- or itch-responding population by expressing GiDREADD, the pain- or itch-related behavioral responses were reduced.

Also, miniscope, a head-mounted fluorescent miniature-microscope invented by UCLA, has been used for imaging the *in vivo* real-time activities of neurons in freely moving mice. I optimized the imaging system of miniscope to improve the quality of recorded images and enhance the reliability of data. By using improved miniscope parts and replacing the surgical instrument, the imaging system got stable, and the images were cleared as inflammation was reduced. I also confirmed the new calcium imaging analysis program, CaImAn, was successfully applied to the miniscope data. Using the optimized miniscope imaging system, I recorded the fluorescent signals from GCaMP6f, one of the genetically encoded calcium indicators (GECIs). The results from miniscope also showed that the overlapping percentage of co-activated ACC neurons tended to be higher when the stimuli were given with 6h interval than 72h interval, which was consistent with the immunohistochemistry data. These results suggested that several ACC neurons were affected by their excitability cycle and tended to be allocated into the pain- or itch-responding populations. At the same time, other activated cells formed inherent ensembles, which were necessary to induce the pain or itch behavioral responses.

Keyword : Anterior cingulate cortex, pain signal processing, itch signal processing, miniscope, genetically encoded calcium indicator, real-time cell activity, calcium imaging

Student number : 2016-29251

Introduction

The signaling pathways of pain and itch have been widely revealed from decades of studies. Remarkably, nociceptive stimuli and pruritic stimuli are known to activate the same dorsal root ganglion (DRG) neurons and they are transmitted through the dorsal horn of the spinal cord and ascended to thalamus through spinothalamic tract (STT) (Davidson and Giesler, 2010). Surgical lesion of the anterolateral funiculus in the spinal cord to alleviate chronic pain abolished itch sensation simultaneously (White and Sweet, 1969), and it was also revealed that the patients who were innately insensitive to pain were insensitive to itch as well (Keele and Armstrong, 1964). They also have been known as counter-stimuli for each other (Szarvas et al., 2003), while itch-inducing agents activate nociceptive primary afferent fibers eliciting both pain and itch sensation (Sikand et al., 2009). From these results, pain and itch have been suggested as germane senses with sharing signaling pathways closely and affecting each other.

Even though an itch-specific pathway was founded (Andrew and Craig, 2001) after the fact, several common brain regions activated by pain and itch stimuli still have been found such as the anterior and posterior cingulate cortex, the anterior and posterior insula, the basal ganglia and the pre-supplementary motor area (Mochizuki et al., 2007). Among those areas, anterior cingulate cortex (ACC) has been reported to be engaged in both pain and itch processing (He et al., 2016; Lu et al., 2018). Two hypotheses were suggested to explain how brain systems evaluate the affective valence of a stimulus: 1) 'affective modules'

hypothesis and 2) 'affective modes' hypothesis (Berridge, 2019). Affective modules hypothesis suggests 'modules', such as a subregion of the brain, projection pathway, a neural population or an individual neuron, process a single affective function permanently. On the contrary, affective modes hypothesis suggests that neural modules can process multiple affective functions. In this point of view, pain and itch are different affective modes processed in the same brain region, ACC. However, it is not uncovered yet how these two different affective modes can be processed in the same region.

Previous studies showed that neurons had excitability cycles (Caracciolo et al., 2018; Herszage et al., 2020; Zhou et al., 2009). Recent experiments with the lateral amygdala (LA) revealed 6h of high excitability phase and 24h of low excitability phase (Josselyn and Frankland, 2018; Rashid et al., 2016). In this study, pain and itch stimuli were provided with 6h or 72h intervals to identify the allocation of the pain- and the itch-responding population was affected by excitability.

Heretofore, neuronal activities have been regarded as the expression of immediate early genes (IEGs). Many experiments have been conducted through detecting IEG protein or mRNA by immunohistochemistry (IHC) or using viral vectors or transgenic mouse lines to express fluorescent proteins under the control of IEG promoters (Cho et al., 2015; Choi et al., 2018; Kawashima et al., 2014; Minatohara et al., 2016; Xiu et al., 2014; Yokose et al., 2017; Zhang et al., 2018). These methods gave us merely indirect evidences for whether the neurons were activated or not. In addition, they should be done after

the subjects were sacrificed, so it was not possible to detect the tendency of neuronal activities via multiple sessions with one subject. In this study, I established an imaging device, called miniscope (Ghosh et al., 2011), which could detect real-time activities of neurons in freely moving mice, to identified the mechanism of subpopulation formation in the ACC. Miniscope is a head-mounted fluorescent microendoscope that images fluorescent signals coming from GECIs which binds to the calcium ion and luminesces fluorescent light after calcium influx induced by the neuronal activities. It made possible to detect the cell activities as a form of fluorescent signals (Oh et al., 2019). I obtained direct evidence of pain- and itch-related neuronal activities through miniscope elicited by the injection of formalin and histamine.

Experimental Procedures

Animal

Fos-tTA x tetO-H2BGFP transgenic mice were generated by crossing Fos-tTA+/- with tetO-H2BGFP+/-. 8~10-week old of Fos-tTA x tetO-H2BGFP and Fos-tTA mice were used for the molecular experiments. Miniscope experiments were performed with 8~10-week old male C57BL/6N mice, and their ACC neurons were recorded at age 14~16 weeks. All mice were housed in a 12-hr light/dark cycle in standard laboratory cages and given *ad libitum* access to food and water. Fos-tTA x tetO-H2BGFP and Fos-tTA mice were exceptionally provided with doxycycline pellets (40g/kg) since they were born and subsequently changed to standard food pellets during dox-off periods. All procedures and animal care followed the regulation and guidelines of the Institutional Animal Care and Use Committees (IACUC) of Seoul National University.

Formalin and histamine injection

1% formalin solution and 40mM histamine solution were always made freshly on the day of injection. Both solutions were diluted with saline and injected with different Hamilton syringes. Mice were anesthetized with isoflurane and shaved in the back of the neck with an electric razor one day before the first injection. On the day of injection, mice were anesthetized with ketamine/xylazine mixture and injected with 10λ of 1% formalin solution or 20λ of 40mM histamine solution. Formalin solution was injected at the hind paw, and histamine

solution was delivered by intradermal injection at the back of the neck.

Experimental procedure with Fos-tTA x tetO-H2BGFP mice

Mice were habituated to handling for 7 days before the first injection. During the last 4 days of habituation, standard food pellets without doxycycline were provided to all mice and changed to doxycycline pellets again after the histamine injection. Histamine was injected after anesthetizing with isoflurane. Mice were injected formalin with 6h or 72h interval. After 90 min from the formalin injection, they were perfused for immunohistochemistry.

Experimental procedure with Fos-tTA mice

AAV1-tetO-hM4Di-P2A-emGFP was injected bilaterally into ACCs (AP +0.7 mm, ML ±0.4 mm, DV −1.7 mm) by stereotaxic surgery (Stoelting Co.). The mice were given 14 days to recover after stereotaxic surgery. One week after the stereotaxic surgery, mice were habituated to handling for 7 days. During the last 4 days of the recovery period, standard food pellets without doxycycline were provided to all the mice. CNO (clozapine-N-oxide) (10mg/kg) or saline as a vehicle was delivered by intraperitoneal injection 30 min before the second injection. For testing the inhibition of itch behavioral response, formalin was injected into one mice group, and histamine was injected into the other mice group as the first injection. Histamine was delivered to all mice as the second injection, and the scratching behaviors were recorded for 30 min for bouts counting. For testing the inhibition of pain behavioral response, one group of mice was injected with formalin

and the other group with histamine as the first injection. All mice were injected with formalin as the second injection, and the hind paw licking behaviors were recorded for 1 hour for counting the duration of licking behavior.

Immunohistochemistry

Mice were anesthetized and transcardially perfused with PBS (0.1 M phosphate buffer, pH 7.4) followed by 4% paraformaldehyde (PFA) in PBS. Brains were collected and immersion-fixed with 4% PFA at 4°C overnight, cryo-protected with 30% sucrose in PBS for two days at 4°C, embedded in an OCT (optimum cutting temperature) compound (Tissue-Tek, Sakura Finetechnical). Coronal sections (40 μm thick) were made using a cryostat, and every 4th section was collected in 50% Glycerol in PBS. Sections were washed with PBS for 5 min three times, incubated with a blocking solution (PBS containing 10% normal goat serum and 0.3% Triton X-100) for 30 min at room temperature, and incubated with rabbit anti-c-Fos antibody (1:250, Santacruz) diluted in the blocking solution for two days at 4°C. Sections were washed with PBS containing 0.3% Triton X-100 (PBST) for 10 min four times, incubated with fluorescent-conjugated secondary antibodies (1:500) diluted in the blocking solution for 2 hours at room temperature, washed with PBST for 10 min four times. After sections were incubated with DAPI (0.2 μg/ml, Invitrogen) in PBS for 10 min at room temperature, sections were transferred onto glass slides and mounted with VECTASHIELD (Vector Laboratories). The sections were imaged with an LSM700 (Carl Zeiss) confocal microscope, and the images were

analyzed using IMARIS software.

Integrated microendoscope

For in vivo 1-photon calcium imaging, I made use of integrated microendoscopes, called miniscopes. The miniscope V3 was used for the experiments. A CMOS imaging sensor (Aptina, MT9V032) was printed on a CMOS imaging sensor PCB (available at https://github.com/daharoni/Miniscope_CMOS_Imaging_Sensor_PCB), while it was connected to a coaxial cable (RG-174/U(50Ω)) by soldering. Luxeon SMD blue LED (P/N LXML-PB01-0030), soldered with excitation LED PCB (printed circuit board), was integrated into the main body structure with CMOS imaging sensor PCB. As optic tools, 5mm Dia. x 12.5mm FL, MgF2 Coated, Achromatic Doublet Lens (Edmund Optics, 49-923), Excitation filter (Chroma, ET470/40×), Emission filter (Chroma, ET525/50m), Dichroic mirror (Chroma, T495lpxr) were also integrated to the main body of the miniscope. 3.0-mm diameter N-BK7 half-ball lens (Edmund Optics, 47-269) was glued with optical adhesive (Edmond Optics, 55-084) and cured by UV. Integrated miniscope was linked to the commutator (PANLINK, PSR-C6) which prevented the coiling of cable.

Stereotaxic surgeries for calcium imaging

For virus injection surgery, mice (8~10 weeks) were anesthetized by intraperitoneal injection of ketamine/xylazine solution and placed on a stereotaxic apparatus (Stoelting Co.). AAV2/1-Ef1α-GCaMP6f was injected into the right ACC (AP +0.7mm, ML +0.25mm, DV -1.9mm)

using a 33-gauge needle with Hamilton syringe. 2 min after the needle tip was placed on 0.1mm below the target location, it returned to the target location and injected 0.5μl of the virus with 0.125μl/min of injection speed. The needle was pulled out slowly 7 min after the injection finished. One week after AAV injection, GRIN lens (graded-index lens) with 2.0mm in diameter (Go!Foton, CLHS200GFT027) was implanted over the ACC. Mice were anesthetized by intraperitoneal injection of ketamine/xylazine solution and positioned in a stereotactic apparatus. The craniotomy for the GRIN lens was 2.0~2.1 mm in diameter so that the gap between the GRIN lens and skull was not almost existed. A cylindrical column of the neocortex was aspirated until the plane that subfornical artery was located with a DNA loading tip flowing saline with a blunt 10ml syringe. After the bleeding stopped, a blood clot was gently removed, and the GRIN lens was implanted (DV 1.7mm) into the hole. The skull was additionally screwed up for structural support. The GRIN lens and screws were fixed with Loctite and dental cement. After curing, biocompatible Silastic elastomer (Kwik-Sil, World Precision Instruments, Berlin Germany) was added around the GRIN lens for protection from scratch. Three weeks after the GRIN lens implant surgery, mice were anesthetized by intraperitoneal injection of ketamine/xylazine solution and positioned in a stereotactic apparatus for a baseplating operation. A baseplate, attached to a miniscope, was placed on the GRIN lens and fixed with dental cement at the angle where the GCaMP6f signal was shown best. The GRIN lens was covered by a cap with screwing on baseplate until the day of calcium imaging.

Miniscope habituation procedures

C57BL/6N mice which underwent whole stereotaxic surgeries were monitored for one week after the baseplating operation. Mice were housed individually in a single cage, and all training and testing were conducted during the light cycle. The mice were habituated to cap removal and miniscope attachment for 5 days without isoflurane anesthesia. Each habituation step endured for 10 minutes after 30 min resting in a rack, and one miniscope was used for one mouse. After habituation to handling during first 2 days, mice underwent miniscope attachment habituation for 2 days, in which miniscopes were attached to baseplates on mice's head with screws and mice were delivered to a new cage and freely moved for 30 sec and miniscopes were detached again and mice were given to the cage and freely moved for 30 sec. This procedure was repeated for 10 min. In the last day of habituation, mice were habituated to an anesthesia box by moving from a cage and an anesthesia box in every 30 sec.

Calcium imaging of freely moving mice

On the day of calcium imaging, mice were rested at a rack for 30 min with attaching a miniscope linked with a commutator. Calcium imaging was performed during the light cycle, and calcium events were recorded by DAQ software (available at https://github.com/daharoni/Miniscope_DAQ_Software) at 30 frames/s of frame rates and with the maximum gain of CMOS sensor. For preventing photobleaching events, LED power was given between 3~10%, and the LED was turned off except for the imaging steps. Each

mouse got the constant LED power during three imaging sessions (0h, 72h, 78h). The commutators were connected to the DAQ board to send the signal from the CMOS to the software on a computer. Before each injection, basal states of neuronal activities were recorded for the first 5 min. Mice were anesthetized with isoflurane and injected histamine into the subcutaneous tissues of the nape neck or formalin into the subcutaneous tissues of the hind paw. After 5-min recovery from isoflurane, calcium signals of itch or pain behavioral responses were imaged for 10 min. After calcium imaging, mice were detached their miniscopes, attached their caps again, and went back to the home racks. In this manner, the three calcium imaging sessions were repeated for one mouse.

Data acquisition, processing, and cell sorting of calcium imaging

The video of calcium transients captured by DAQ software and DAQ hardware (Labmaker or Sierra Circuits, v3.2) were saved as AVI file extension formats. Those videos were processed by CaImAn program, which is the open-source library for calcium imaging data analysis based on the CNMF algorithm (Giovannucci et al., 2019). Initially, movies of each session were integrated into a single video. The integrated videos went through several analyzing steps, including pre-processing and neural activity identification. Pre-processing consisted of 3 steps: motion correction, source extraction, and activity deconvolution. Using CaImAn, motion correction was performed by registering each data frame to a set of overlapping FOV (field of view) patches. Source extraction was performed to demix overlapping

sources from each other and the background neuropil signals. Finally, in the activity deconvolution step, each neural activity from the identified source was detrended to remove the photobleaching effect and deconvolved from the fluorescence traces. The pre-processed videos got through the component detection step, which used 4-layer CNN (convolutional neural network), and those components in videos from multiple sessions were registered by the CaImAn.

Results

Improvement of miniscope body parts and surgery steps optimized the quality of recorded images.

For reliable calcium imaging data, the recording system's stability and the quality of recorded images should be ensured for multi-session recording in one mouse. For stabilizing the imaging system, the original miniscope body was modified in some ways. First, to minimize image trembling during free movement of mice, I re-designed the structure of baseplates with three types: one with a thick bottom, one with an additional wall, and one with both (Figure 2A). The leading cause of image trembling was the tilted state of miniscope fixed onto the baseplate. The miniscopes were tilted because the original baseplates' structure was too weak to be bent, and the baseplates were easily deformed as miniscope fixation with screws was repeated. To prevent the deformation of the baseplate and make the image statically, the durability of three versions of new baseplates were teste. Only the baseplate version with the thick bottom and additional wall was strong enough to endure repeated fixations over 30 times and the miniscopes could be fixed almost straightly on them (Figure 2B).

The original coaxial cable, which had a silicon rubber outer sheet, was too soft to withstand the torsion force and deliver it to the commutator. The cable was entangled first rather than spinning, which made the commutator could not release the torsion force, ending up with the shortened cable length that disrupted the mice's behavior. For

finding a coaxial cable with proper tension, several products were tested with mice. When using the coaxial cable with a PVC (polyvinyl chloride) outer sheet, mice can move freely and raise their head easily (Figure 2C). Additionally, the connection between the main body and coaxial cable was strengthened by adding an epoxy bond (Figure 2D), which had been easily broken when just connected by soldering. It authentically averted disconnection error during miniscope recording and made the LED power steadily. The optical filters were also fixed with cellophane tape not to move inside the main body (Figure 2D) which had caused a wobble of the light field in ROI (region of interest). It reduced noises in fluorescent signals and allowed the cell-activity analysis to be more reliable. Furthermore, the most crucial element to enhance the image quality was the GRIN lens implantation surgery. I used a loading tip to aspirate the brain tissue rather than a blunt needle. It reduced the inflammation and bleeding, in turn, made the images to be clear. As a result, the quality of miniscope images was much improved; even the dendrite could be identified, and it became possible to distinguish a cytosol and nucleus in a cell body (Figure 3).

Surgery conditions for ACC miniscope imaging and data analysis with CaImAn were established.

There was no previous study that recorded the ACC region by miniscopes. So, ACC surgery for miniscope imaging was established first. As human synapsin (hsyn) promoter was found not to be expressed in ACC layer 2/3 (Figure 4A), Ef1α promoter was used to express

GCaMP6f (Figure 4B), a GECI that visualized calcium influx in cytosol of neurons as a form of fluorescent signals. The subfornical artery was established as a landmark for aspirating the ACC tissue, positioning in the middle depth of the ACC region (Figure 4C). The layer 2/3 of ACC was discriminated from layer 5 by monitoring with miniscopes, and imaged subsequently (Figure 4D, E). Various algorithms had been introduced to analyze the calcium signal, such as CNMF, CNMF-E, M1NPIPE. Among those, I analyzed recorded images by a CNMF algorithm-based program called CaImAn, which detected the neurons and their GCaMP6f signals after pre-processing steps (Figure 5). I confirmed that CaImAn successfully analyzed the CA1 and ACC images as catching a bunch of cells (mean: 165.6 (n=13) in ACC layer 2/3) with fewer noise signals (Figure 6).

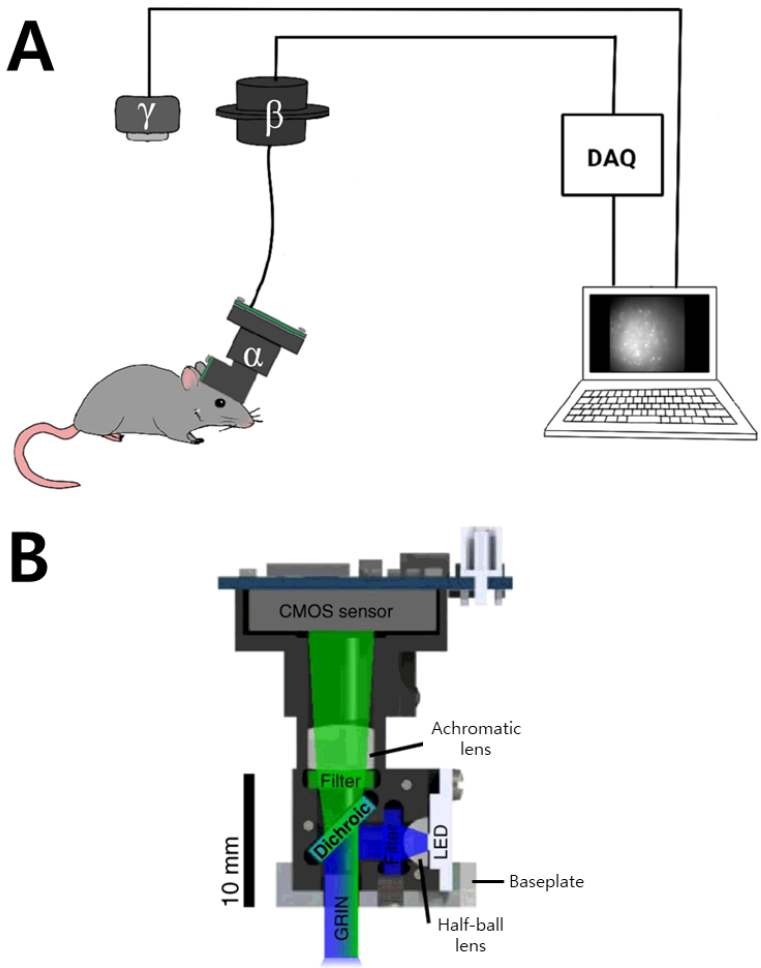

Figure 1. UCLA miniscope system

(A) The schematic image of the miniscope imaging system. DAQ hardware received the calcium signals from miniscope and behavioral information simultaneously and passed them on to the DAQ software. α: miniscope, β: commutator, preventing the twisting of coaxial cable by rotating, γ: behavior camera (B) The structure of miniscope. The blue-ray from the LED passed the filter that only passed blue light, and was reflected by a dichroic mirror. It went to the brain tissue through a GRIN lens, then induced the emission of green light from the GECI, such as GCaMP6f. Green lights passed the dichromatic mirror because of their incident angle, and then through the green light filter and achromatic lens, their image fell on the CMOS sensor.

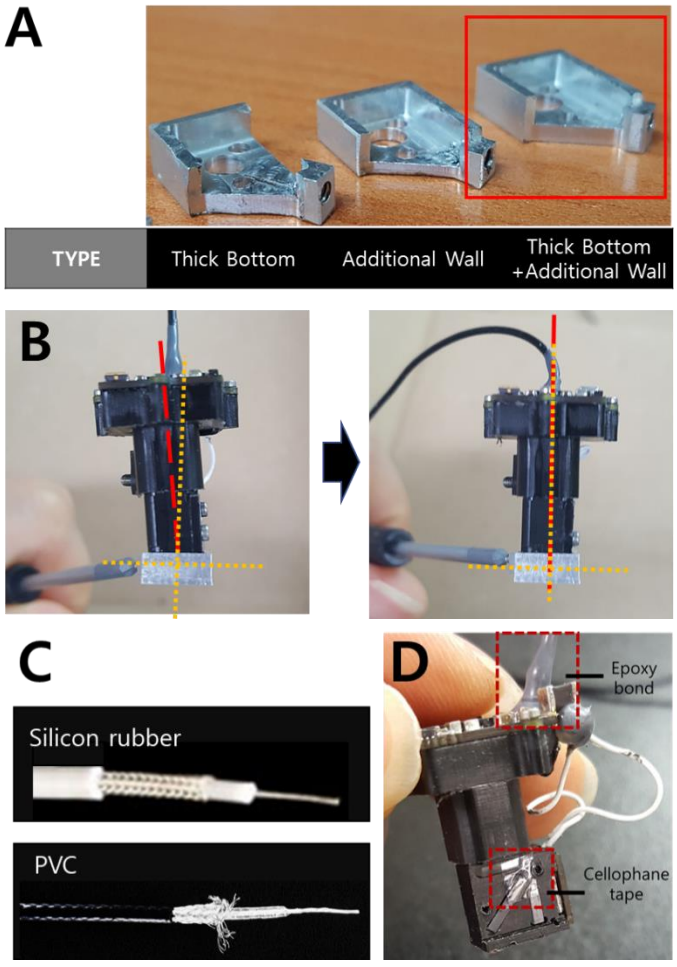

Figure 2. Improved parts of the miniscope for optimal imaging with moving animal.

(A) Baseplates were newly designed into three types which had a 1.5-fold thick bottom or additional wall on the side part or both of them. (B) Miniscopes were fixed straightly on the baseplate version with a thick bottom and additional wall. (C) The coaxial cable made of a silicon rubber outer sheet (top) was replaced with the one made of a PVC outer sheet (bottom). (D) Epoxy bond was added to strengthen the connection between PCB and coaxial cable, and cellophane tape held the optical filters not to tremble inside the main body.

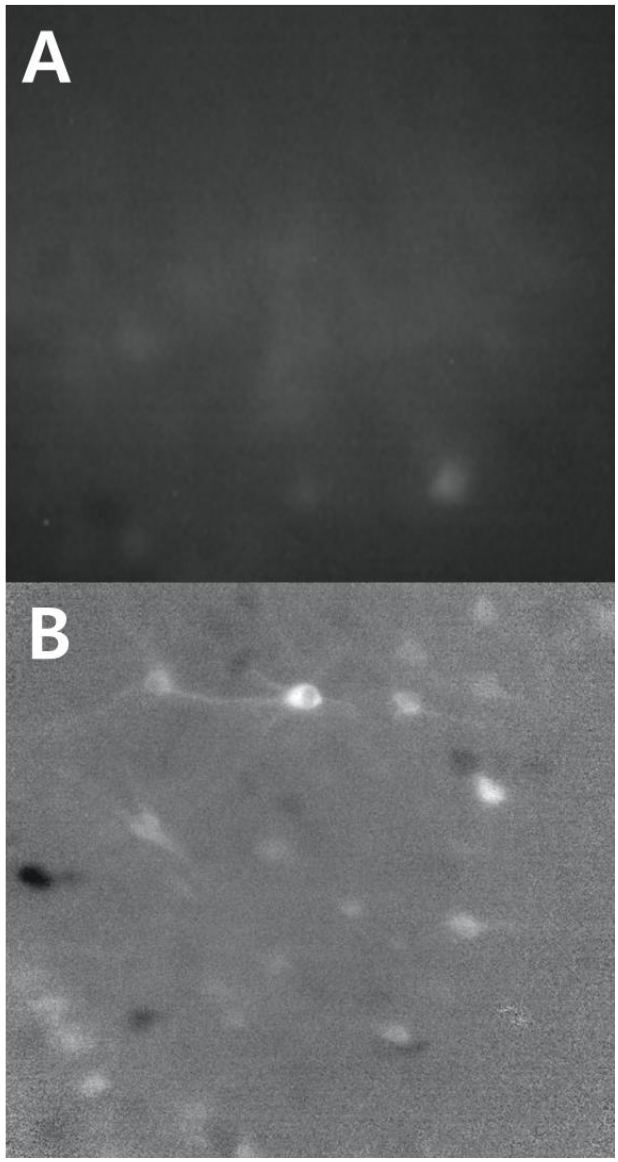

Figure 3. Improved raw image quality with optimized miniscope system in CA1.

(A) and (B) are the snapshots of dF/F videos recorded before and after the optimization of the miniscope recording system. While the cells were not clear and the cell boundaries could be found barely in (A), The dendrites and even the boundaries between nuclei and cytosols could be distinguishable.

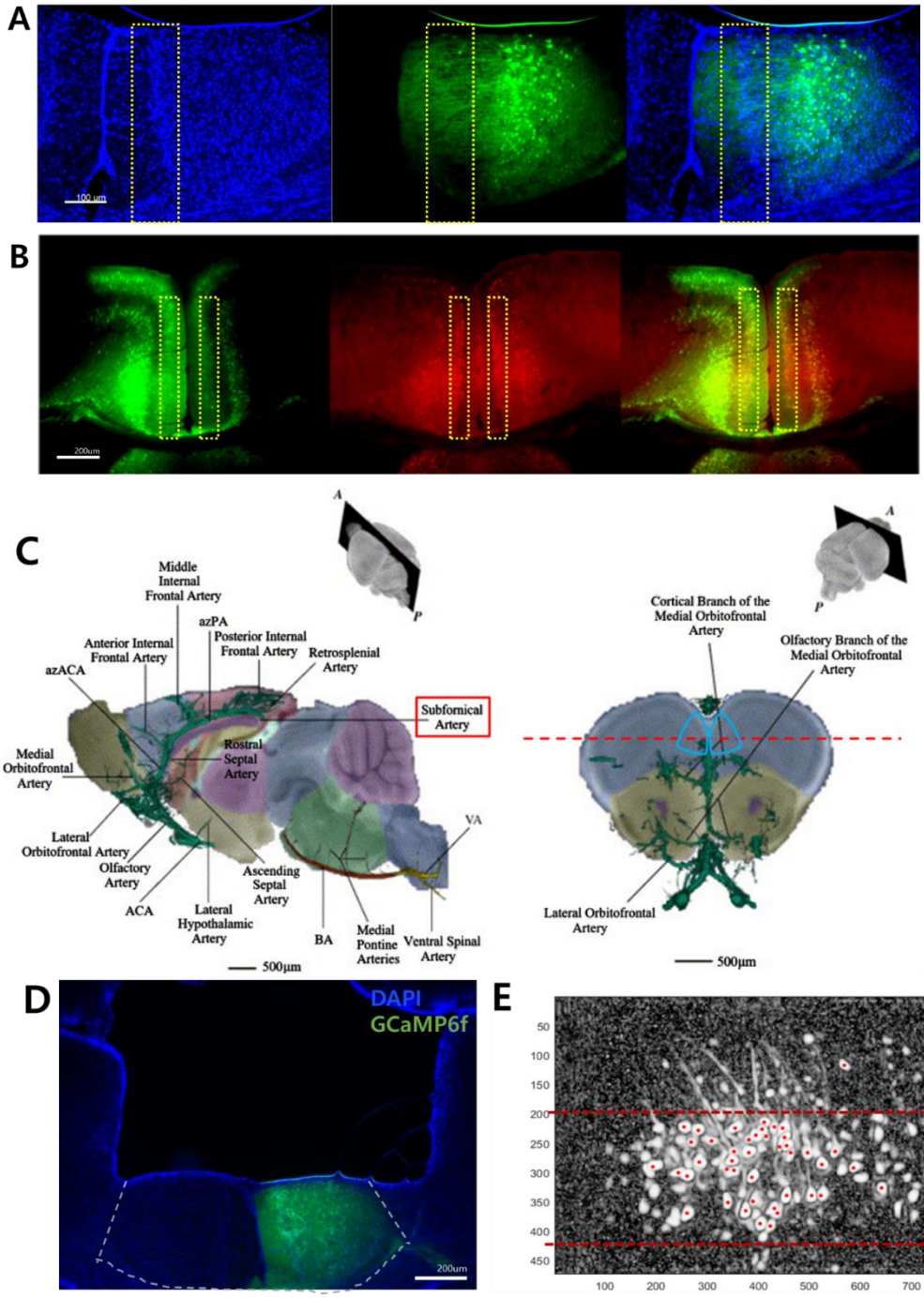
A
100μm
B
200μm
C
A
P
Middle Internal Frontal Artery
azPA
Posterior Internal Frontal Artery
Anterior Internal Frontal Artery
azACA
Retrosplenial Artery
Subfornical Artery
Rostral Septal Artery
Medial Orbitofrontal Artery
Lateral Orbitofrontal Artery
Olfactory Artery
ACA
Lateral Hypothalamic Artery
Ascending Septal Artery
BA
Medial Pontine Arteries
Ventral Spinal Artery
VA
500μm
A
P
Cortical Branch of the Medial Orbitofrontal Artery
Olfactory Branch of the Medial Orbitofrontal Artery
Lateral Orbitofrontal Artery
500μm
D
DAPI
GCaMP6f
200um
E
50
100
150
200
250
300
350
400
450
100
200
300
400
500
600
700

Figure 4. Miniscope surgery conditions in ACC

(A) GCaM6f was not expressed in layer 2/3 of ACC under the control of the hsyn promoter. (blue: DAPI, green: hsyn-GCaMP6f) (B) GCaM6f was expressed in layer 2/3 of ACC under the control of the Ef1α promoter. (green: Ef1a-GCaMP6f, red: CaMKIIα-mCherry) (C) The location of the subfornical artery that traversed the middle of the ACC region (Dorr et al., 2007) was chosen for the landmark of suction. The region marked with the blue line is ACC, and the red horizontal dash line is the plane the Subfornical artery lies. The brain tissue was aspirated till the plane. (D) The brain image of a mouse which underwent the miniscope surgery. (E) The image of miniscope recording after cell detecting analysis of the (D) mouse. The region between the two red dash lines is ACC layer 2/3. Some of the dendrites reached toward the ACC layer 5.

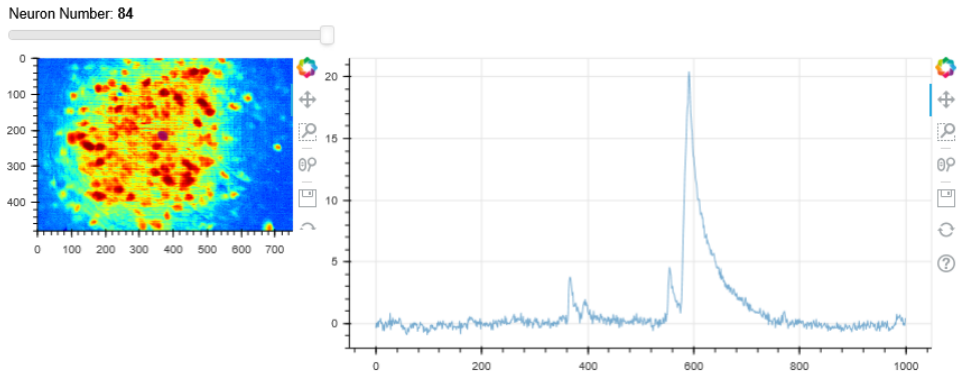

Figure 5. CaImAn system establishment

The CA1 video sample recorded by the optimized miniscope system was successfully analyzed with CaImAn program. CaImAn results showed the detected cells as a heat map and the fluorescent signal graph of each detected cell.

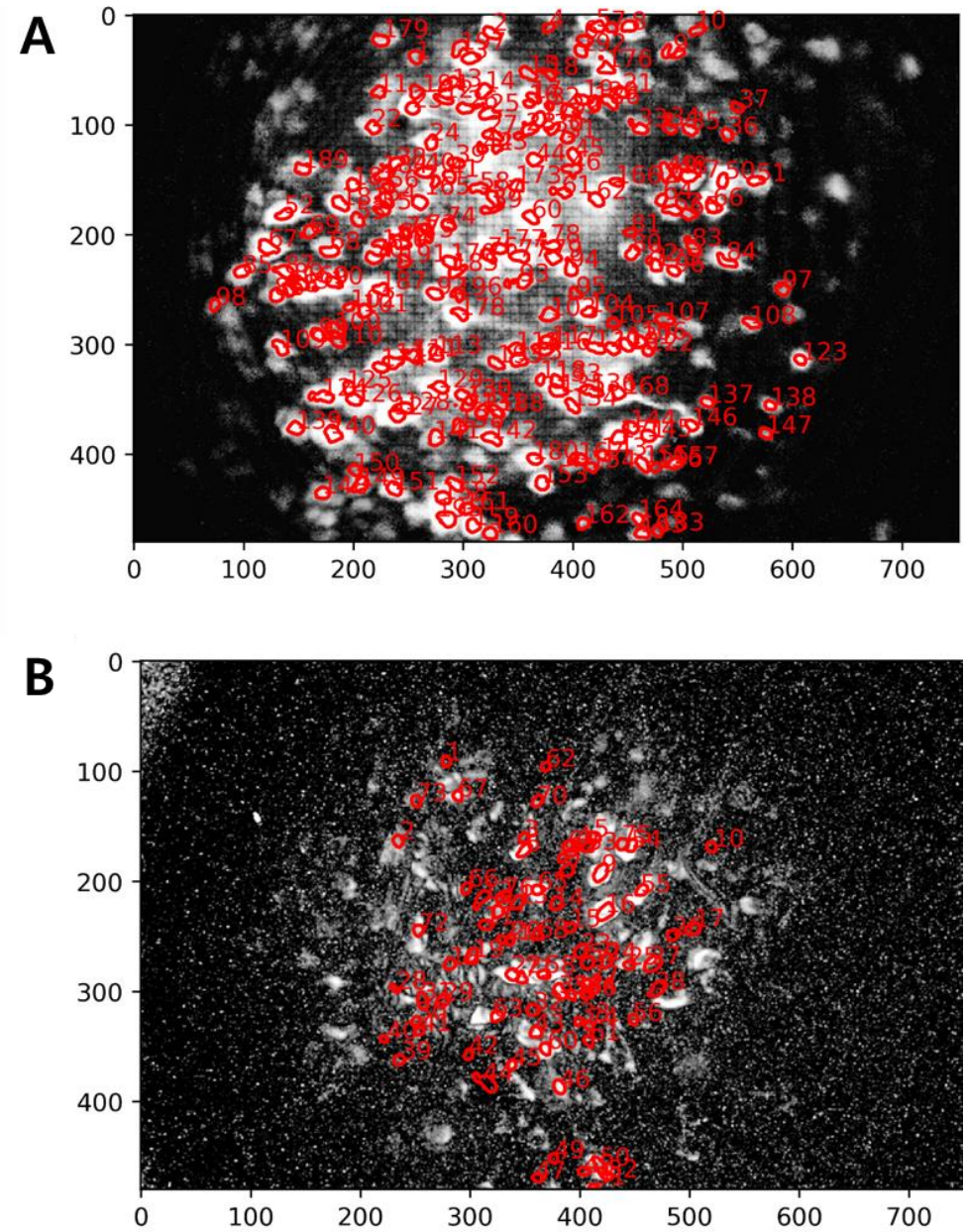

Figure 6. The results of cell detection analysis by CaImAn

More cells were detected in better quality images with the optimized miniscope system. In these images, 196 cells were detected in CA1, and 76 cells were detected in the ACC layer 2/3.

Excitability of neurons affected to allocating population responding to pain and itch stimuli.

To understand how the ACC responded to pain and itch stimuli, Fos-tTA x tetO-H2BGFP transgenic mice were divided into two groups and injected histamine and formalin solutions sequentially with 6h or 72 intervals (Figure 7A). tTA was expressed by the c-fos promoter on the dox-off time point. The activated cells to histamine were labeled with H2BGFP under the control of tTA expression, while the activated cells to formalin were labeled with c-fos antibodies by IHC (Figure 7B). As a result, the pain- and itch- responding cells were found to be highly co-activated at 6h interval than 72h (Figure 7C-F). These results indicate that the activities of some ACC neurons to pain or itch are affected by their excitabilities.

Pain- and itch-responding populations were necessary to induce pain and itch behavioral responses.

To identify whether the pain- and itch-responding cells were necessary to induce the pain and itch behavioral responses, AAV1-tetO-hM4Di-P2A-emeraldGFP was injected into Fos-tTA transgenic mice, and the activated cells by formalin or histamine were labeled with GiDREADD under the control of the c-fos promoter. After 72h, the CNO for inhibiting GiDREADD-labelled neurons or saline as a control was injected, followed by formalin or histamine injection. The mice in which CNO inhibited the pain-responding cells showed less behavioral responses to pain than the mice in which the cells responding to

histamine were inhibited or those injected saline (Figure 8A). Also, the mice in which the itch-responding cells were inhibited showed less behavioral responses to itch than those in which the pain-responding cells were inhibited or those injected saline (Figure 8B, D), while the expression levels of hM4Di were not significantly different among all groups (Figure 8C, E). These results indicate that some of the ACC neurons form the inherent neuron groups responding to pain or itch after the pain or itch stimuli, which are necessary to induce pain or itch behavioral responses.

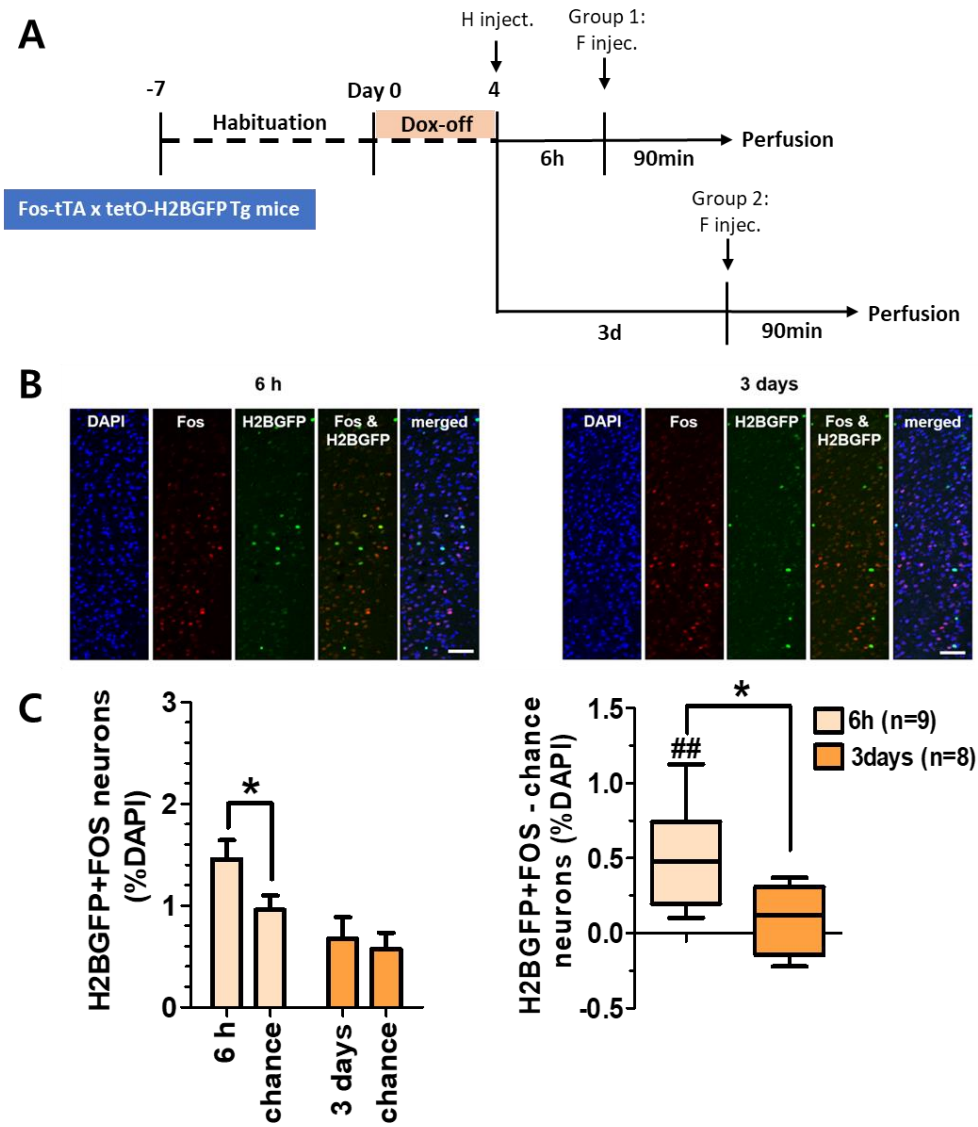

Figure 7. Overlapping rates of pain and itch responding populations were affected by excitability.

(A) The scheme of histamine and formalin injection and perfusion experiments (B) The colocalization of Fos-expressing cells (red) and H2BGFP-expressing cells (green) with 6h and 3d interval. (C) The overlapping rate between H2BGFP and Fos was significantly higher than the chance level in the 6h interval. (D) The value of the overlapping rate excluded chance level was significantly different between 6h and 72h interval.

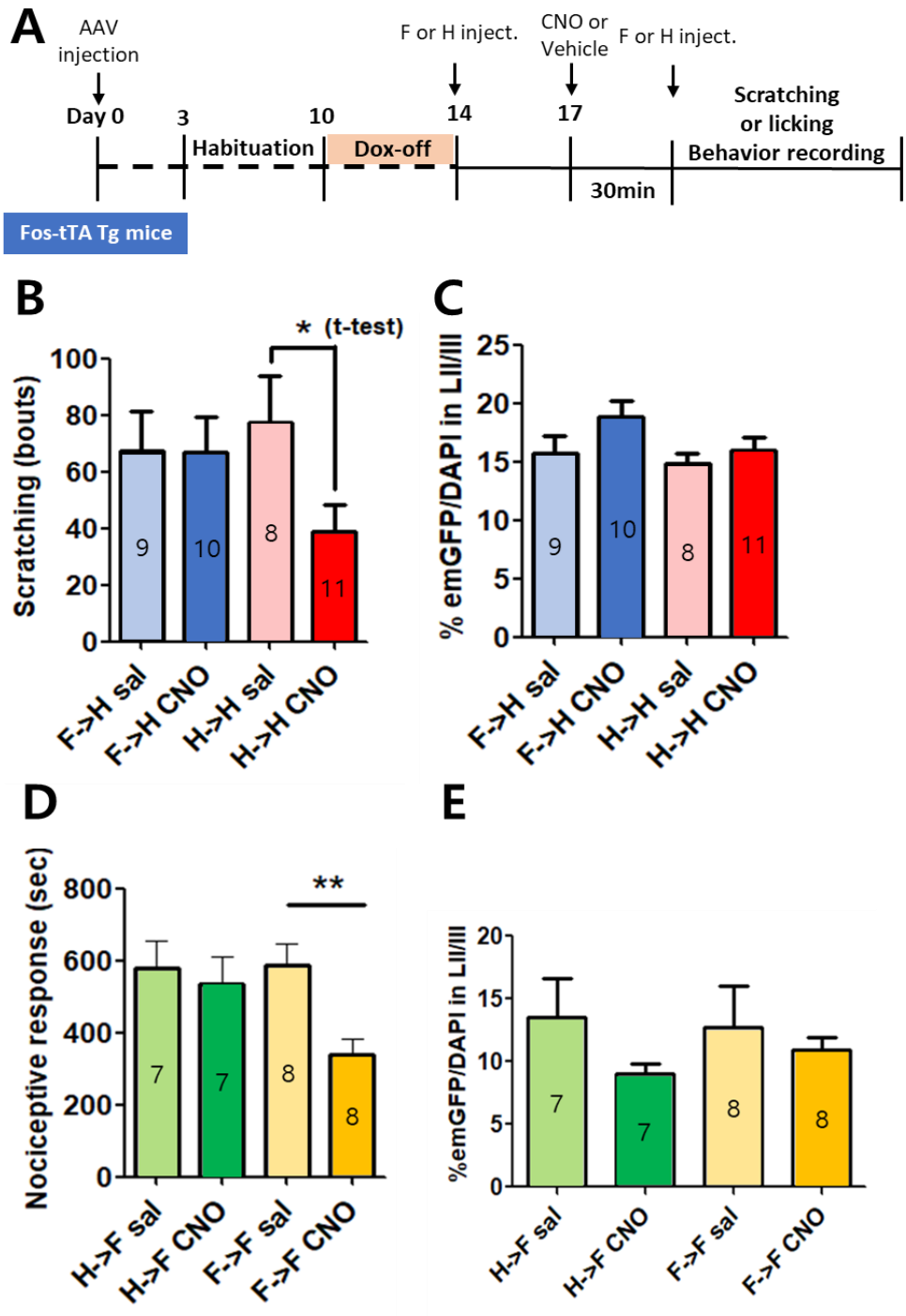
A
AAV injection
Day 0
3
Habituation
10
Dox-off
14
F or H inject.
17
CNO or Vehicle
F or H inject.
30min
Scratching or licking Behavior recording
Fos-tTA Tg mice
B
* (t-test)
Scratching (bouts)
100
80
60
40
20
0
9
10
8
11
F->H sal
F->H CNO
H->H sal
H->H CNO
C
% emGFP/DAPI in LII/III
25
20
15
10
5
0
9
10
8
11
F->H sal
F->H CNO
H->H sal
H->H CNO
D
**
Nociceptive response (sec)
800
600
400
200
0
7
7
8
8
H->F sal
H->F CNO
F->F sal
F->F CNO
E
%emGFP/DAPI in LII/III
20
15
10
5
0
7
7
8
8
H->F sal
H->F CNO
F->F sal
F->F CNO

Figure 8. Pain and itch behaviors inhibited by GiDREADD.

(A) The scheme of experiments. AAV1-tetO-hM4Di-P2A-emeraldGFP was injected to Fos-tTA mice. After the virus was expressed for 2 weeks and 3 days of the dox-off period, the first injection of formalin or histamine was given, and pain- or itch-responding population expressed hM4Di and emeraldGFP proteins during 3 days. After inhibiting those populations with CNO, one mice group was given the same stimulus, and the other mice group were given the other stimulus compared to the first injection. (B) and (D) the mice groups that received the pain or itch stimuli after inhibiting the population responding to the same stimuli showed significantly lower behavioral responses. (C) and (E) showed that the number of cells that expressed emeraldGFP was not different significantly.

Activated cells to pain or itch stimuli imaged by miniscopes were more overlapped between groups with the 6h interval than 72h.

To investigate whether the results from the transgenic mice and IHC reproduce the real cell activity patterns, I imaged the real-time activities of ACC neurons with the optimized miniscope system. The 4 groups of mice were divided according to the series of solutions they were injected: 1) histamine-histamine-histamine (H-H-H) group, 2) formalin-formalin-formalin (F-F-F) group, 3) histamine-formalin-histamine (H-F-H) group and 4) formalin-histamine-formalin (F-H-F) group. The first two stimuli were given with a 6h interval, and the last stimulus was given at 72h after the second stimulus (Figure 9A). Five-day habituation steps with miniscopes were conducted before the imaging to reduce the isoflurane anesthesia once and minimize the recovery time from it. The neuronal activities of the basal state and formalin or histamine responding state were imaged and analyzed by the CaImAn program. The overlapping percentage of co-activated cells in sessions was calculated by aligning all detected cells from every two sessions. The cells having the same location coordinate were overlapped and regarded as a corresponding cell. It was not significant but tended that the overlapping rates between the 6h interval were higher than those between 72h interval (Figure 9B). I compared the ratio of the overlapping rate of 6h and 72 intervals with the ratio of the overlapping rate of 6h and 72 intervals in the basal state, representing the endogenous excitability cycle in the ACC region. No group was significantly different from the chance level, which indicates that there is a tendency for ACC neurons to be affected by excitability. These

results were consistent with the previous results and proved that miniscope data would be able to validate the results from transgenic mice and IHC data.

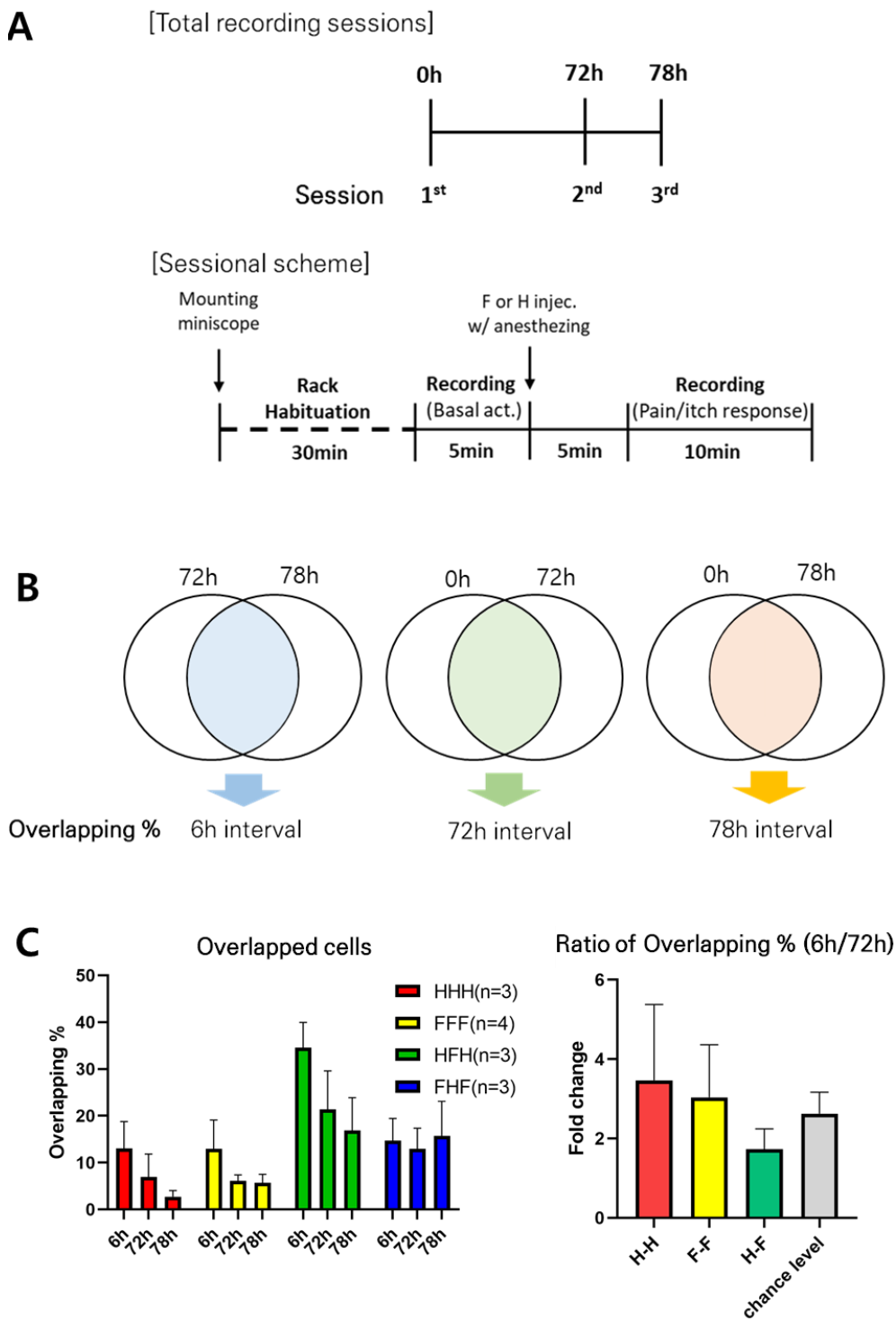
A
[Total recording sessions]
0h
72h
78h
Session
1st
2nd
3rd
[Sessional scheme]
Mounting miniscope
F or H injec. w/ anesthezing
Rack Habituation
30min
Recording (Basal act.)
5min
5min
Recording (Pain/itch response)
10min
B
72h
78h
0h
72h
0h
78h
Overlapping %
6h interval
72h interval
78h interval
C
Overlapped cells
Overlapping %
HHH(n=3)
FFF(n=4)
HFH(n=3)
FHF(n=3)
6h
72h
78h
Ratio of Overlapping % (6h/72h)
Fold change
H-H
F-F
H-F
chance level

Figure 9. Miniscope results of overlapped cells in pain- and itch-responding populations.

(A) The scheme of miniscope recording. Each mouse underwent 3 sessions of recording at 0h, 72h and 78h, and in each session, after miniscope mounting without anesthetizing and habituation at a rack, basal activity was recorded for 5 min, and formalin or histamine was injected with isoflurane anesthesia. Mice recovered for 5 min, and the activity responding to formalin or histamine was recorded for 10 min. (B) The overlapping percentage of 6h interval was calculated by counting the overlapped cells between 72h and 78h recording images. The overlapping percentages of 72h and 78h interval were calculated in the same way. (C) Overlapping rate with 6h interval tended to be higher than 72h and 78h intervals. Also, all ratios between 6h and 72h overlapping percentages were not significantly different from the chance level.

Discussion

Recently, many researchers have tried to get real-time neuronal activity with microendoscopes such as miniscope or Inscopix. Inscopix's microendoscopes are commonly used these days because of their stable imaging system and convenient data analysis program. However, their high cost limits the accessibility to many laboratories. Therefore, the researchers who even chose Inscopix's had to use just one or two microendoscopes for multiple mice. This limitation would matter because the same focal plane should be ensured when imaging the multiple sessions. Even though they provide the focus-matching tools in their program, it always has to be adjusted whenever the subjects are changed if the number of available microendoscopes is less than that of mice. In opposite, miniscopes developed by UCLA have a lower cost than those of Inscopix. So, it is possible to make enough number of miniscopes and assign one miniscope to one mouse. However, users have to assemble it from parts to a whole set of machinery by soldering, even the major demerit of miniscope was the lack of stability of the imaging system. It has been a colossal restraint to record multiple sessions with a subject. The coaxial cables were bent too easily, ending up with shortened lines restricting the movement of mice, and the connection between PCB and coaxial cable was broken often by mice moving during imaging. The quality of images was also too poor to capture a sufficient number of neurons and to get reliable

fluorescent signal data as shown in the previous research articles (Chen et al., 2020; Ghandour et al., 2019; Nelson et al., 2019). In this report, I overcame the shortcomings of the original miniscope system by improving the durability of the baseplate and the connection between PCB and coaxial cable. Also, I enhanced the image quality by replacing the surgical instrument and reducing inflammation. Many researchers were guided to use the dexamethasone and amoxicillin to reduce the inflammation, however, I found the most important thing was the sophisticated surgery steps rather than the anti-inflammatory drug injection after the fact. Eventually, examining the CaImAn program could be utilized with recorded images from miniscope with less computing power allowed the miniscope system to be applied easier to any laboratory condition.

The manipulation of neuropathic pain and chronic itch has been an essential theme in neurobiology and medical science. It has been known that somatic senses have unique pathways. However, pain and itch intimately shared their signaling ascending pathways and brain areas (White and Sweet, 1969), although eliciting different behavioral responses. Several previous articles showed that the ACC was activated with pain or itch stimuli, nevertheless, no result examined how the ACC could process two different somatosensory signals in one region. This study showed that inhibiting the pain- and itch-responding cells could decrease the pain- and itch-related behaviors, and simultaneously, pain- and itch-responding populations were highly overlapped with 6h

interval than 72h. The latter founding seems to be the result of excitability that increased in the activated neurons by prior stimuli and enhanced the probability to be activated to the subsequent stimulus (Yiu et al., 2014). In conclusion, these results suggest that some neurons are pain- or itch-specific neurons, which were able to be examined by inhibiting them, and some other neurons in the ACC are activated by their excitability cycle. The latter population could not be examined because if they were inhibited, the other neurons that had the second-high excitability would take place to be activated. Also, these results examined the existence of ACC neurons activated by both pain and itch stimuli, which supported the affective mode hypothesis rather than the affective module hypothesis. It will provide insights on explaining the way of the brain's affective mode processing.

Indeed, there were several studies related to memory formation which proved that the results from existing cell activity detection, such as capturing IEG expressing neurons with IHC, transgenic mouse lines, or delivering viral vector containing fluorescent protein genes with IEG promoters, were consistent with the real-time neuronal activity pattern representing the calcium signals acquired with microendoscopes methods (Cai et al., 2016). This study also examined the tendency of pain- and itch-activity patterns obtained by miniscopes was consistent with the results from IHC and transgenic mouse line. Although it was not significant statistically, the tendency might be examined later by adding a supplementary number of subjects and data. In addition, it

can be suggested that miniscope can replace the previous labeling system of activated neurons with transgenic mice or IHC. These investigations might galvanize the research trying to find the cell activities in real-time using miniscope and derive more direct evidence of neuronal activities. Additional miniscope data analysis of activation pattern, action potential frequency, or population coding will provide more specific insights on pain and itch processing and on pain- or itch-specific remedies.

References

Andrew, D., and Craig, A.D. (2001). Spinothalamic lamina I neurons selectively sensitive to histamine: a central neural pathway for itch. Nat. Neurosci. *4*, 72-77.

Berridge, K.C. (2019). Affective valence in the brain: modules or modes? Nat. Rev. Neurosci. *20*, 225-234.

Cai, D.J., Aharoni, D., Shuman, T., Shobe, J., Biane, J., Song, W., Wei, B., Veshkini, M., La-Vu, M., Lou, J., et al. (2016). A shared neural ensemble links distinct contextual memories encoded close in time. Nature *534*, 115-118.

Caracciolo, L., Marosi, M., Mazzitelli, J., Latifi, S., Sano, Y., Galvan, L., Kawaguchi, R., Holley, S., Levine, M.S., Coppola, G., et al. (2018). CREB controls cortical circuit plasticity and functional recovery after stroke. Nat. Commun. *9*, 2250.

Cho, J., Yu, N.-K., Choi, J.-H., Sim, S.-E., Kang, S.J., Kwak, C., Lee, S.-W., Kim, J., Choi, D.I., Kim, V.N., et al. (2015). Multiple repressive mechanisms in the hippocampus during memory formation. Science *350*, 82-87.

Choi, J.-H., Sim, S.-E., Kim, J., Choi, D.I., Oh, J., Ye, S., Lee, J., Kim, T., Ko, H.-G., Lim, C.-S., et al. (2018). Interregional synaptic maps among engram cells underlie memory formation. Science *360*, 430-435.

Davidson, S., and Giesler, G.J. (2010). The multiple pathways for itch

and their interactions with pain. Trends Neurosci. *33*, 550–558.

Dorr, A., Sled, J.G., and Kabani, N. (2007). Three-dimensional cerebral vasculature of the CBA mouse brain: A magnetic resonance imaging and micro computed tomography study. NeuroImage *35*, 1409–1423.

Ghosh, K.K., Burns, L.D., Cocker, E.D., Nimmerjahn, A., Ziv, Y., Gamal, A.E., and Schnitzer, M.J. (2011). Miniaturized integration of a fluorescence microscope. Nat. Methods *8*, 871–878.

Giovannucci, A., Friedrich, J., Gunn, P., Kalfon, J., Brown, B.L., Koay, S.A., Taxidis, J., Najafi, F., Gauthier, J.L., Zhou, P., et al. (2019). CaImAn an open source tool for scalable calcium imaging data analysis. ELife *8*, e38173.

He, Z.-G., Zhang, D.-Y., Liu, S.-G., Feng, L., Feng, M.-H., and Xiang, H.-B. (2016). Neural circuits of pain and itch processing involved in anterior cingulate cortex. Int J Clin Exp Med *9*, 22976–22984.

Herszage, J., Dayan, E., Sharon, H., and Censor, N. (2020). Explaining Individual Differences in Motor Behavior by Intrinsic Functional Connectivity and Corticospinal Excitability. Front. Neurosci. *14*.

Josselyn, S.A., and Frankland, P.W. (2018). Memory Allocation: Mechanisms and Function. Annu. Rev. Neurosci. *41*, 389–413.

Kawashima, T., Okuno, H., and Bito, H. (2014). A new era for functional labeling of neurons: activity-dependent promoters have come of age. Front. Neural Circuits *8*.

Keele, C.A., and Armstrong, D. (1964). Substances producing pain and itch (E. Arnold).

Lu, Y.-C., Wang, Y.-J., Lu, B., Chen, M., Zheng, P., and Liu, J.-G. (2018). ACC to Dorsal Medial Striatum Inputs Modulate Histaminergic Itch Sensation. J. Neurosci. Off. J. Soc. Neurosci. *38*, 3823-3839.

Minatohara, K., Akiyoshi, M., and Okuno, H. (2016). Role of Immediate-Early Genes in Synaptic Plasticity and Neuronal Ensembles Underlying the Memory Trace. Front. Mol. Neurosci. *8*.

Mochizuki, H., Sadato, N., Saito, D.N., Toyoda, H., Tashiro, M., Okamura, N., and Yanai, K. (2007). Neural correlates of perceptual difference between itching and pain: A human fMRI study. NeuroImage *36*, 706-717.

Oh, J., Lee, C., and Kaang, and B.-K. (2019). Imaging and analysis of genetically encoded calcium indicators linking neural circuits and behaviors. Korean J. Physiol. Pharmacol. *23*, 237-249.

Rashid, A.J., Yan, C., Mercaldo, V., Hsiang, H.-L. (Liz), Park, S., Cole, C.J., Cristofaro, A.D., Yu, J., Ramakrishnan, C., Lee, S.Y., et al. (2016). Competition between engrams influences fear memory formation and recall. Science *353*, 383-387.

Sikand, P., Shimada, S.G., Green, B.G., and LaMotte, R.H. (2009). Similar itch and nociceptive sensations evoked by punctate cutaneous application of capsaicin, histamine and cowhage. PAIN® *144*, 66-75.

Szarvas, S., Harmon, D., and Murphy, D. (2003). Neuraxial opioid-induced pruritus: a review. J. Clin. Anesth. *15*, 234-239.

White, J.C., and Sweet, W.H. (1969). Pain and the neurosurgeon: a forty-year experience (CC Thomas).

Xiu, J., Zhang, Q., Zhou, T., Zhou, T., Chen, Y., and Hu, H. (2014). Visualizing an emotional valence map in the limbic forebrain by TAI-FISH. Nat. Neurosci. *17*, 1552-1559.

Yokose, J., Okubo-Suzuki, R., Nomoto, M., Ohkawa, N., Nishizono, H., Suzuki, A., Matsuo, M., Tsujimura, S., Takahashi, Y., Nagase, M., et al. (2017). Overlapping memory trace indispensable for linking, but not recalling, individual memories. Science *355*, 398-403.

Zhang, Q., He, Q., Wang, J., Fu, C., and Hu, H. (2018). Use of TAI-FISH to visualize neural ensembles activated by multiple stimuli. Nat. Protoc. *13*, 118-133.

Zhou, Y., Won, J., Karlsson, M.G., Zhou, M., Rogerson, T., Balaji, J., Neve, R., Poirazi, P., and Silva, A.J. (2009). CREB regulates excitability and the allocation of memory to subsets of neurons in the amygdala. Nat. Neurosci. *12*, 1438-1443.

국 문 초 록

통증과 가려움은 서로 다른 정동감각이며 전달 경로와 두 감각을 처리하는 뇌 영역이 긴밀하게 관련되어 있으며, 그 중에서도 전두대상피질은 통증과 가려움 모두를 처리하는 것으로 잘 알려져 있다. 뇌가 여러 체감각들을 서로 다른 것으로 인지하는지에 관해 여러 가설들이 제시되었으나 지금까지 한 영역에서 두 체감각이 어떻게 처리되는지에 관해서는 연구된 바 없었다. 본 연구에서는 쥐에 6시간 간격으로 가려움과 통증 자극을 주었을 때 두 자극 모두에 반응하는 전두대상피질영역의 뉴런들의 비율이 72시간 간격으로 자극이 주어졌을 때보다 높은 것을 확인하였다. 또한 통증 또는 가려움 자극에 반응하는 뉴런 집단에 GiDREADD를 발현시킴으로써 억제하였을 때 통증 또는 가려움 관련 행동이 감소하는 것을 확인하였다.

머리탑재형 초소형 형광현미경인 미니스콥은 UCLA에서 개발되었으며, 움직이는 쥐에서 실시간으로 뉴런의 활성을 촬영하기 위해 사용된다. 본 연구에서는 미니스콥 부품들을 개선하고 수술 도구를 대체함으로써 촬영 시스템의 안정성을 높이고 수술로 인한 뇌조직의 염증을 줄임으로써 깨끗한 영상을 얻을 수 있었으며 최적화된 미니스콥의 촬영 시스템을 통해 뉴런 활성 영상의 질을 높이고 데이터의 신뢰도를 높였다. 또한, 새로운 칼슘 이미징 분석 프로그램인 CaImAn이 미니스콥으로 얻어진 데이터에 성공적으로 적용되는 것을 확인하였다. 이렇게 구축된 시스템을 이용하여 활성화된 뉴런 내부로 유입되는 칼슘과 결합했을 때 형광을 발현하는 단백질의 일종인 GCaMP6f 단백질의 형광 신호를 촬영하였다. 미니스콥을 통해 얻어진 결과 또한 면역조직화학법으로 얻어진 결과와 마찬가지로 6시간 간격으로 통증 또는 가려움 자극이 주어질 경우 두 자극

모두에 반응한 뉴런들의 수가 72시간 간격이었을 때 보다 많은 경향을 보이는 것을 확인하였다. 이러한 결과들은 일부 전두대상피질 뉴런들은 흥분성 주기에 영향을 받아 통증 또는 가려움에 반응하는 뉴런 집단에 속하는 경향이 있으며 다른 일부 전두대상피질 뉴런들은 통증 또는 가려움에 특이적으로 반응하는 고유의 뉴런 집단을 형성하여 통증 또는 가려움 행동 반응 유도에 필요하다는 것을 제시한다.